The Volume Regulation Graph versus the Ejection Fraction as Metrics of Left Ventricular Performance in Heart Failure with and without a Preserved Ejection Fraction: A Mathematical Model Study

Theo J.C. Faes and Peter L.M. Kerkhof

Department of Physics and Medical Technology, VU-University Medical Center, Amsterdam, The Netherlands.

Supplementary Issue: Heart Failure: An Exploration of Recent Advances in Research and Treatment

ABSTRACT: In left ventricular heart failure, often a distinction is made between patients with a reduced and a preserved ejection fraction (EF). As EF is a composite metric of both the end-diastolic volume (EDV) and the end-systolic ventricular volume (ESV), the lucidity of the EF is sometimes questioned. As an alternative, the ESV–EDV graph is advocated. This study identifies the dependence of the EF and the EDV–ESV graph on the major determinants of ventricular performance. Numerical simulations were made using a model of the systemic circulation, consisting of an atrium–ventricle valves combination; a simple constant pressure as venous filling system; and a three-element Windkessel extended with a venous system. ESV–EDV graphs and EFs were calculated using this model while varying one by one the filling pressure, diastolic and systolic ventricular elastances, and diastolic pressure in the aorta. In conclusion, the ESV–EDV graph separates between diastolic and systolic dysfunction while the EF encompasses these two pathologies. Therefore, the ESV–EDV graph can provide an advantage over EF in heart failure studies.

KEYWORDS: heart failure, ejection fraction, volume regulation graph, cardiovascular model

SUPPLEMENT: Heart Failure: An Exploration of Recent Advances in Research and Treatment

CITATION: Faes and Kerkhof. The Volume Regulation Graph versus the Ejection Fraction as Metrics of Left Ventricular Performance in Heart Failure with and without a Preserved Ejection Fraction: A Mathematical Model Study. *Clinical Medicine Insights: Cardiology* 2015:9(S1) 73–91 doi: 10.4137/CMC.S18748.

RECEIVED: December 02, 2014. **RESUBMITTED:** March 15, 2015. **ACCEPTED FOR PUBLICATION:** March 18, 2015.

ACADEMIC EDITOR: Thomas E. Vanhecke, Editor in Chief

TYPE: Original Research

FUNDING: Authors disclose no funding sources.

COMPETING INTERESTS: Authors disclose no potential conflicts of interest.

CORRESPONDENCE: tjc.faes@vumc.nl, plm.kerkhof@vumc.nl

Introduction

Left ventricular (LV) heart failure (HF) is a prevalent cardiac syndrome, characterized by altered LV size and shape, elevated filling pressure, increased biomarkers, specific risk factors, plus a wide variety of symptoms and signs.[1] In HF often a distinction is made between patients on the basis of their ejection fraction (EF). About half of all HF patients present with a reduced EF (denoted as HFrEF), while the others show a preserved EF (denoted as HFpEF). In order to distinguish between both groups, the following criteria are commonly used[2]: an EF larger than or equal to 50% and an end-diastolic ventricular volume index (EDVI) smaller than 97 mL/m^2 are required for HFpEF, while an EF smaller than 50% is set for HFrEF. For both groups, the gold standard[3] of an end-diastolic ventricular pressure (EDP) larger than 16 mmHg (millimeter mercury) is an additional requirement. Thus, the combination of LV pressure and volume plays a prominent role in the analysis of HF phenotypes.

EF is the pivotal measure in the current classification scheme.[1] However, the EF is both a quantitative measure that relates the ejected stroke volume (SV) to the EDV, as a percentage, as well as a qualitative measure that summarizes the complex ventricular interplay with the venous system during the filling phase (preload) and the arterial system during the ejection phase (afterload) within that same single metric. As a result, the EF as a preferred measure of ventricular performance is often questioned.[1,4–8] To quote Robotham, for instance: "Thus, EF, although a relatively simple measure that is intuitively easily comprehended, is an extremely complex parameter describing the entire cardiovascular system and requires additional study".[5] Concentrating more specifically on HF, it is noted that despite recent insights into the recognition of the importance of LV reverse remodeling in HF, many clinicians do not consider simple measurements of LV structure (ie, LV volume) in their routine clinical decision-making process.[9] Instead, they often rely on EF when making decisions about medical and surgical treatment options.[9]

Rather than combining the end-diastolic volume (EDV) and the end-systolic volume (ESV) of the ventricle in the single percentage of the EF, some authors advocate to study ventricular performance on the basis of both LV volumes by

using a graph with the EDV on the abscissa and the ESV on the ordinate.[1,10] Recently, a linear relationship

$$\mathrm{ESV} = q + s\ \mathrm{EDV} \tag{1}$$

with slope s and intercept q, was reported for a study concerning 34 HFpEF patients and 29 HFrEF patients (Fig. 1). Each group clustered around its own regression line with a quite small overlap in the ESV versus EDV graph and, moreover, the slopes of these two lines were reported to be significantly different.[8] To be specific, Kerkhof reports a slope of 0.35 in HFpEF versus a slope of 0.80 in HFrEF ($P < 0.0004$) and an intercept of –6.97 mL/m^2 in HFpEF versus –19.24 mL/m^2 in HFrEF.[8] Clearly, the EF and the slope of the regression line in the EDV–ESV graph are related, namely

$$\mathrm{EF} = \frac{\mathrm{EDV} - \mathrm{ESV}}{\mathrm{EDV}} = \frac{\mathrm{EDV} - \left(q + s\,EDV\right)}{\mathrm{EDV}} = 1 - \left(s + \frac{q}{EDV}\right) \tag{2}$$

For a vanishing intercept ($q = 0$), this relation shows that EF equals 1 minus the slope s in the ESV–EDV graph. As expected, Figure 1 shows a steeper regression line for the HFrEF group (EF <50%) than for the HFpEF group (EF ≥50%). However for a nonvanishing intercept ($q \neq 0$), the relation between EF and s may be strongly influenced by EDV. Indeed, from Figure 1 significant nonvanishing intercepts for both groups can be inferred, and hence, the presumed simple relation between EF and s is seriously distorted by prevailing values of EDV. And, therefore, the EF and the ESV–EDV graph must be considered as different and noncomparable metrics representing the volumes EDV and ESV.

Clearly, the EF and the ESV–EDV graph appear to reflect quite differently the relationship between EDV and ESV and, with that, the (patho-)physiological mechanisms of ventricular performance in the HF spectrum. Therefore, this study aims to identify the dependence of the EF and the EDV–ESV graph on the major determinants of ventricular performance, in particular, for the phenotypes HFpEF and HFrEF, and

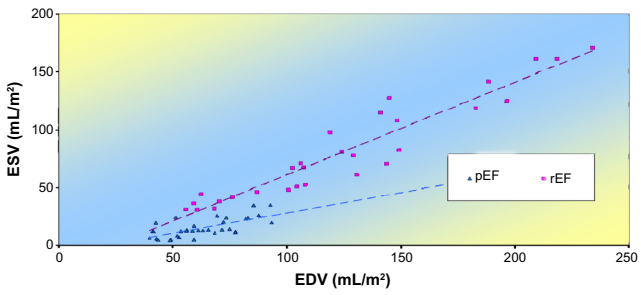

Figure 1. Graph of end-systolic volume index (ESVI) versus end-diastolic volume index (EDVI), illustrating the distinct patterns for heart failure patients with preserved (pEF, $n = 34$) and reduced EF (rEF, $n = 29$). Volumes are normalized for body surface area. Diagram slightly modified from Kerkhof et al.[8]

preferable by using a simple mathematical model of the cardiovascular system. Using a monoventricular model, first the major determinants are identified and second the dependence of the EF and the EDV–ESV graph on these determinants is calculated.

Methods

Cardiovascular model. Our model of the cardiovascular system consists of the systemic circulation only, with the atrium and ventricle being filled from a simple constant pressure source and the heart ejecting into a circulatory system. The model is discussed in detail in Appendix A.

In each simulation run, the model provides results on EDV, ESV, SV, EF, and end-diastolic pressure EDP. The outcomes are classified as follows (2):

- HFpEF, if EF ≥50%, EDV <175 mL and EDP >16 mmHg;
- HFrEF, if EF <50% and EDP >16 mmHg.

and any result of a simulation run outside of these constraints was neglected.

In order to be able to guide the model simulations, one aspect of the model needs explanation here. The single-sided cardiac unit consists of a left atrium and a LV together with the mitral and aortic valves. For both the atrium and the ventricle, the well-known Suga–Sagawa elastance model is used for the pressure–volume characteristics.[11] This model reads as:

$$P(t) = E(t)\left\{V(t) - V_0\right\} \tag{3}$$

where $P(t)$ is the time-dependent ventricular pressure (mmHg), $V(t)$ the time-dependent ventricular volume (mL), V_0 the (extrapolated) ventricular volume (mL) at zero ventricular pressure, and $E(t)$ the time-dependent ventricular elastance (mmHg/mL). Note that this relation holds for every point in time during the cardiac cycle and, in particular, for the end-systolic moment, in which case the relation is referred to as the end-systolic pressure–volume relationship. For the LV, Senzaki et al provide a formulation enabling to express the elastance as a function of time, namely in terms of a Fourier series.[12] We will use the Suga–Sagawa elastance model to investigate the major determinants of EDV and ESV and, by the same token, those of the EF (see below in this section).

Major determinants. In order to identify the major determinates of EF and the EDV–ESV graph, we reason as follows:

$$\mathrm{EF} = \frac{\mathrm{EDV} - \mathrm{ESV}}{\mathrm{EDV}} = 1 - \frac{\mathrm{ESV}}{\mathrm{EDV}} = 1 - \frac{\min\{V(t)\}}{\max\{V(t)\}} \tag{4}$$

where t represents time (s) and $V(t)$ is the time-dependent ventricular volume (mL). Clearly, EDV is the maximum of

$V(t)$ during diastole (denoted as $\max\{V(t)\}$) and ESV is the minimum of $V(t)$ during systole (denoted as $\min\{V(t)\}$).

In order to relate the EDV and ESV to ventricular elastance, Suga–Sagawa's pressure–volume relation $P(t) = E(t)\{V(t) - V_0\}$ is used.[13] Upon rewriting the Suga–Sagawa's relation, the EDV is

$$\mathrm{EDV} \overset{(1)}{=} \max\{V(t)\} \overset{(2)}{=} \max\left\{\frac{P(t)}{E(t)} + V_0\right\} \overset{(3)}{=} \max\left\{\frac{P(t)}{E(t)}\right\} + V_0 \overset{(4)}{\leq} \frac{\max\{P(t)\}}{\min\{E(t)\}} + V_0 \overset{(5)}{=} \frac{P_{FILL}}{E_{MIN}} + V_0 \overset{(6)}{=} \frac{P_{FILL}}{E_{MIN}}\left(1 + \frac{E_{MIN}V_0}{P_{FILL}}\right) \quad (5)$$

with the following rationales at the numbered equal signs: (1) EDV is the maximum ventricular volume during diastole; (2) a rewritten form of Suga–Sagawa's pressure–volume relation; (3) the maximum of the sum of a ratio and a constant equals the maximum of the ratio summed to the constant; (4) by application of the general rule that the maximum of a ratio is smaller than or equal to the ratio of the maximum of the fraction's numerator divided by the minimum of the fraction's denominator; (5) the maximum pressure of the ventricle during diastole is the filling pressure P_{FILL} (mmHg) (neglecting the atrial kick) and the minimum ventricular elastance is defined as E_{MIN} (mmHg/mL); (6) rewriting in a more convenient form by factoring the term $P_{\mathrm{FILL}}/E_{\mathrm{MIN}}$.

Likewise, and *mutatis mutandis*, the ESV is found

$$ESV \overset{(1)}{=} \min\{V(t)\} \overset{(2)}{=} \min\left\{\frac{P(t)}{E(t)} + V_0\right\} \overset{(3)}{=} \min\left\{\frac{P(t)}{E(t)}\right\} + V_0 \overset{(4)}{\geq} \frac{\min\{P(t)\}}{\max\{E(t)\}} + V_0 \overset{(5)}{=} \frac{P_{DIAS}}{E_{MAX}} + V_0 \overset{(6)}{=} \frac{P_{DIAS}}{E_{MAX}}\left(1 + \frac{E_{MAX}V_0}{P_{DIAS}}\right) \quad (6)$$

with the following rationales at the numbered equal signs: (1) ESV is the minimum ventricular volume during systole; (2) a rewritten form of Suga–Sagawa's pressure–volume relation; (3) the minimum of the sum of a ratio and a constant equals the minimum of the ratio summed to the constant; (4) by application of the general rule that the minimum of a ratio is larger than or equal to the ratio of the minimum of the fraction's numerator divided by the maximum of the fraction's denominator; (5) the minimum pressure of the ventricle during ejection is equal to the end-diastolic pressure in the aorta, ie, P_{DIAS} (mmHg) and E_{MAX} (mmHg/mL) is the maximum ventricular elastance and referred to as the maximum systolic elastance; (6) rewriting in a more convenient form by factoring the term $P_{\mathrm{DIAS/MAX}}$.

The ratio of ESV to EDV is found by substitution of Eqns. (5) and (6). To be specific:

$$\frac{\mathrm{ESV}}{\mathrm{EDV}} \geq \frac{\frac{P_{DIAS}}{E_{MAX}} + V_0}{\frac{P_{FILL}}{E_{MIN}} + V_0} = \frac{\left(\frac{P_{DIAS}}{E_{MAX}}\right)\left(1 + \frac{E_{MAX}}{P_{DIAS}}V_0\right)}{\left(\frac{P_{FILL}}{E_{MIN}}\right)\left(1 + \frac{E_{MIN}}{P_{FILL}}V_0\right)} \approx \frac{\left(\frac{P_{DIAS}}{E_{MAX}}\right)}{\left(\frac{P_{FILL}}{E_{MIN}}\right)} \quad (7)$$

and the EF follows by substitution of Eq. (7) into Eq. (4):

$$\mathrm{EF} = \frac{\mathrm{EDV} - \mathrm{ESV}}{\mathrm{EDV}} = 1 - \frac{\mathrm{ESV}}{\mathrm{EDV}} \leq 1 - \frac{\frac{P_{DIAS}}{E_{MAX}} + V_0}{\frac{P_{FILL}}{E_{MIN}} + V_0} = 1 - \frac{\left(\frac{P_{DIAS}}{E_{MAX}}\right)}{\left(\frac{P_{FILL}}{E_{MIN}}\right)} \frac{\left(1 + \frac{E_{MAX}}{P_{DIAS}}V_0\right)}{\left(1 + \frac{E_{MIN}}{P_{FILL}}V_0\right)} \approx 1 - \frac{\left(\frac{P_{DIAS}}{E_{MAX}}\right)}{\left(\frac{P_{FILL}}{E_{MIN}}\right)} \quad (8)$$

In Eqns. (7) and (8) the last approximation holds, only if V_0 vanishes (ie, $V_0 = 0$) or if the numerical values of the ratios $E_{\mathrm{MAX}}/P_{\mathrm{DIAS}}$ and $E_{\mathrm{MIN}}/P_{\mathrm{FILL}}$ are of equal size because, in either way, the terms $(1 + V_0E_{\mathrm{MAX}}/P_{\mathrm{DIAS}})$ and $(1 + V_0E_{\mathrm{MIN}}/P_{\mathrm{FILL}})$ cancel. Typical values are calculated from Table 1. In HFpEF: $E_{\mathrm{MAX}}/P_{\mathrm{DIAS}} = 0.11\ \mathrm{mL}^{-1}$ and $E_{\mathrm{MIN}}/P_{\mathrm{FILL}} = 0.01$; in HFrEF: $E_{\mathrm{MAX}}/P_{\mathrm{DIAS}} = 0.02\ \mathrm{mL}^{-1}$ and $E_{\mathrm{MIN}}/P_{\mathrm{FILL}} = 0.005\ \mathrm{mL}^{-1}$. Notice that E_{MAX} in Table 1 is estimated assuming that $V_0 = 0$ and that, therefore, these values are rough estimates only. So, these numerical values indicate that the terms $(1 + V_0E_{\mathrm{MAX}}/P_{\mathrm{DIAS}})$ and $(1 + V_0E_{\mathrm{MIN}}/P_{\mathrm{FILL}})$ only cancel in the unlikely case of a vanishing V_0. Therefore, the final approximations in Eqns. (7) and (8) are somewhat questionable.

To summarize these mathematical results:

1. There is no reason to assume that V_0 vanishes in this model simulation study.
2. The major determinants of the EDV (see Eq. (5)) are the ratio of the filling pressure (P_{FILL}) over the elastance during diastole (E_{MIN}) and the zero-pressure volume of the ventricle (V_0). Note that the ratio $P_{\mathrm{FILL}}/E_{\mathrm{MIN}}$ can be interpreted as the preload normalized to the diastolic ventricular elastance.
3. The major determinants of the ESV (see Eq. (6)) are the ratio of the diastolic aortic pressure (P_{DIAS}) over the elastance during systole (E_{MAX}) and the zero-pressure volume of the ventricle (V_0). Note that the ratio $P_{\mathrm{DIAS}}/E_{\mathrm{MAX}}$ can be interpreted as an indicator of the afterload normalized to the systolic ventricular elastance.
4. Because the EF and the ESV–EDV graphs are defined in terms of the EDV and ESV, both the EF and the ESV–EDV graphs share common determinants. Note that this sharing of determinants does not imply the equivalence of the EF and the ESV–EDV graph. See the Introduction for the relation between EF and the slope of the ESV–EDV graph.
5. The result for the volume ratio of ESV over EDV (Eq. (7)) predicts a linear relation in the ESV–EDV graph with a small or even vanishing intercept and slope smaller than 1 and, moreover, infers an elastance-normalized afterload $P_{\mathrm{DIAS}}/E_{\mathrm{MAX}}$ smaller than the elastance-normalized preload $P_{\mathrm{FILL}}/E_{\mathrm{MIN}}$.

Table 1. Hemodynamic data of HFpEF and HFrEF patient groups; average values (standard deviation).

	HFPEF (N = 26)	HFREF (N = 27)	*P*-VALUE
Ventricular pressures			
LVP peak (mmHg)	174.12 (38.19)	138.00 (24.47)	<0.00007
LVEDP (mmHg)	22.88 (4.63)	22.26 (3.71)	ns
Aortic pressures			
Systolic (mmHg)	169.62 (36.51)	137.33 (23.14)	<0.0002
Diastolic (mmHg)	73.54 (16.05)	72.33 (12.84)	ns
PP (mmHg)	96.08 (28.69)	65.00 (21.74)	<0.00003
MAP (mmHg)	110.04 (21.58)	96.22 (13.82)	<0.005
Volumes			
SVI (mL/m^2)	47.67 (10.62)	43.29 (16.49)	ns
SV (mL)	85.81	77.92	
EDVI (mL/m^2)	63.04	124.97	
EDV (mL)	113.47	224.95	
ESV (mL)	27.66	147.02	
Flows and heart rate			
Heart rate (bpm)	67.15 (11.22)	85.67 (14.93)	<0.000003
CI (L/m^2.min)	3.20 (0.86)	3.61 (1.33)	ns
CO (L/min)	5.76	6.50	
Characteristic parameters			
R (mmHg·s/mL)	1.15	0.89	
C indexed for BSA (mL/mmHg.m^2)	0.52 (0.15)	0.72 (0.33)	0.004
C (mL/mmHg.m^2)	0.94	1.30	
E_{MAX} indexed for BSA (mmHg.m^2/mL)	14.36 (9.35)	2.03 (1.27)	<0.00001
E_{max} (mmHg/mL)	7.98	1.13	
E_{MIN} (mmHg/mL)	0.20	0.10	
E_a indexed for BSA (mmHg.m^2/mL)	3.43 (0.99)	3.33 (1.48)	ns
E_a (mmHg/mL)	1.91	1.85	
Coupling index *k*	4.32 (2.75)	0.63 (0.31)	<0.000001

Notes: Modified from Kerkhof et al.[8,16] In particular, the highly significant group differences in LVP peak, systolic and pulse pressure, and E_{MAX} – possibly indicating a difference in systolic ventricular performance – and, moreover, differences in HR and circulatory parameters R and C – possibly indicating a neurohumoral compensation in HFrEF. The original volumetric data was indexed for body surface area (BSA). Nonindexed mean values were calculated using a BSA of 1.8 m^2. Moreover, the mean flow resistance R was calculated from MAP over CO; ESV was calculated from EDV and SV; E_{MIN} was calculated as LVEDP/EDV.

Abbreviations: ns, not significant; LVP peak, maximum left ventricular pressure; LVEDP, left ventricular end-diastolic pressure; PP, pulse pressure; MAP, mean arterial pressure; CO, cardiac output; CI, cardiac index; R, flow resistance; C, arterial compliance; E_{MAX} , maximum of ventricular elastance (assuming $V_0 = 0$); E_a the arterial elastance, and *k* is the coupling index (ie, E_{MAX}/E_a).

On the basis of these findings, we decided to study the EF and the ESV–EDV plot by varying the abovementioned determinants (P_{DIAS}, E_{MAX}, P_{FILL}, E_{MIN}, and V_0) in order to identify major factors contributing to the distinct LV volume patterns manifested in HFpEF relative to HFrEF (cf. Fig. 1).

Results

Figure 2 shows the simulation results of pressures, volumes, and elastances as a function of time and, additionally, the LV pressure–volume and elastance–volume loops for a control and the HFpEF and HFrEF groups.

Note that the model parameters are chosen such that the latter two groups represent values as given in Table 1. The control represents the values provided by Katz,[14] ie, filling pressure of 7 mmHg, maximum ventricular pressure of 120 mmHg, end-systolic pressure of 95 mmHg, end-diastolic pressure in the aorta of 80 mmHg, EDV 120 mL including atrial kick of 20 mL, end-systolic volume 50 mL, and an EF of 60%. Note in particular the large difference in the maximum ventricular elastance in the three simulations. The simulations closely resemble the data in Table 1 and those reported by Katz, with the exception of the pressures in HFrEF.

Note that, the elastance–pressure plot and the pressure–volume plot for the ventricle in Figure 2 clearly show the constant value of the elastance during diastole and, consequently, a linear dependence of the pressure on the volume.

Figures 3–7 show the changes in the cardiovascular model when one of the model parameters is varied. To be specific, in Figures 3, 4, 5, 6, and 7, respectively, the variable varied is the diastolic elastance (E_{MIN}), the filling pressure, the systolic elastance, the capillary resistance (R_C), and finally, the zero-pressure ventricular volume (V_0). In each of these figures, the following is shown:

- First and second rows show the LV pressure–volume and elastance–volume loops, respectively.
- Third row shows the arterial and ventricular pressures and the ventricular volumes, the SV, and the EF as functions of the running variable.
- Fourth row shows the ESV–EDV plot (with slope and intercept of regression line) and the Starling curve with SV as function of EDV.

See the legends for information on the range of the running variable.

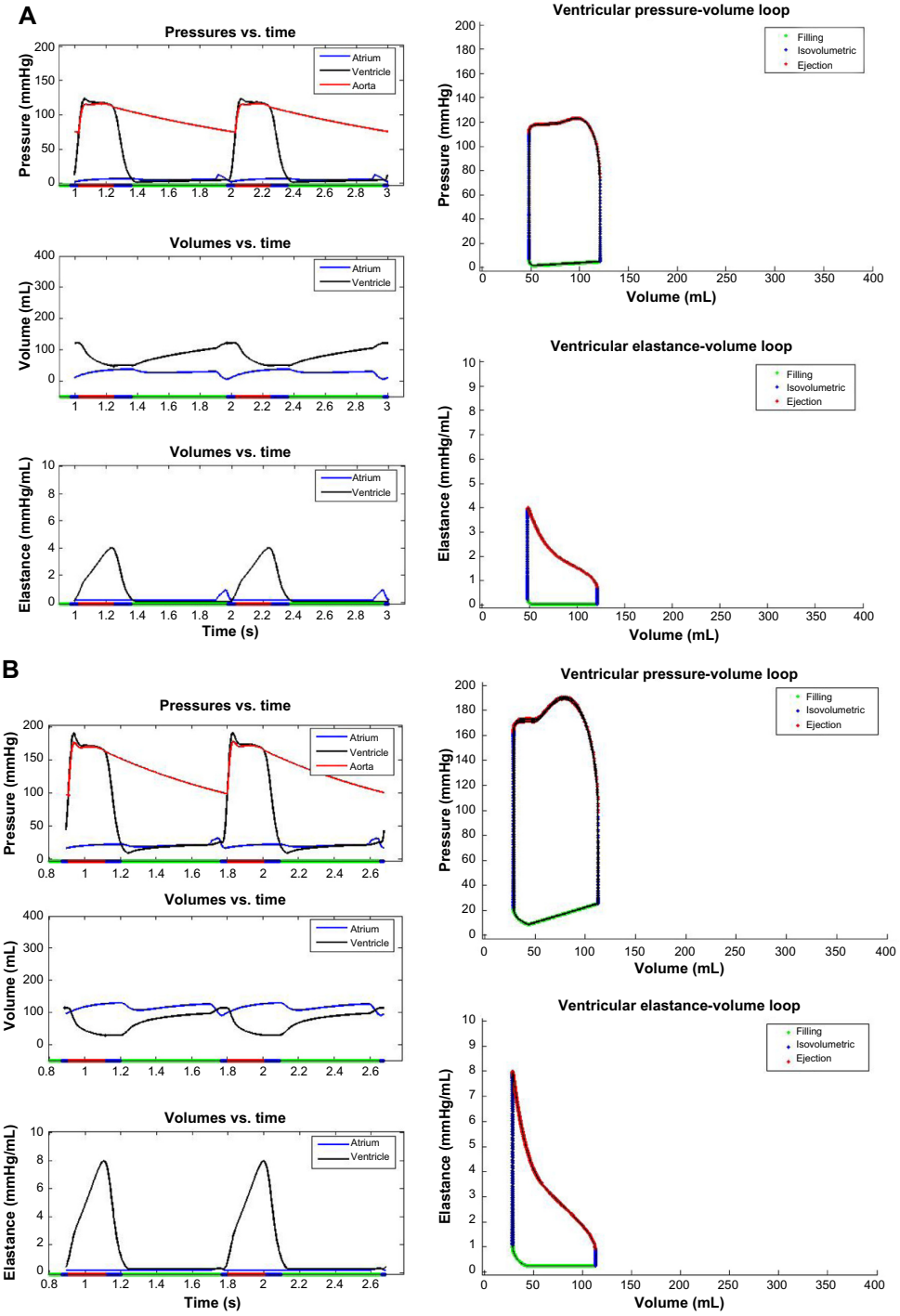

Figure 2. (*Continued*)

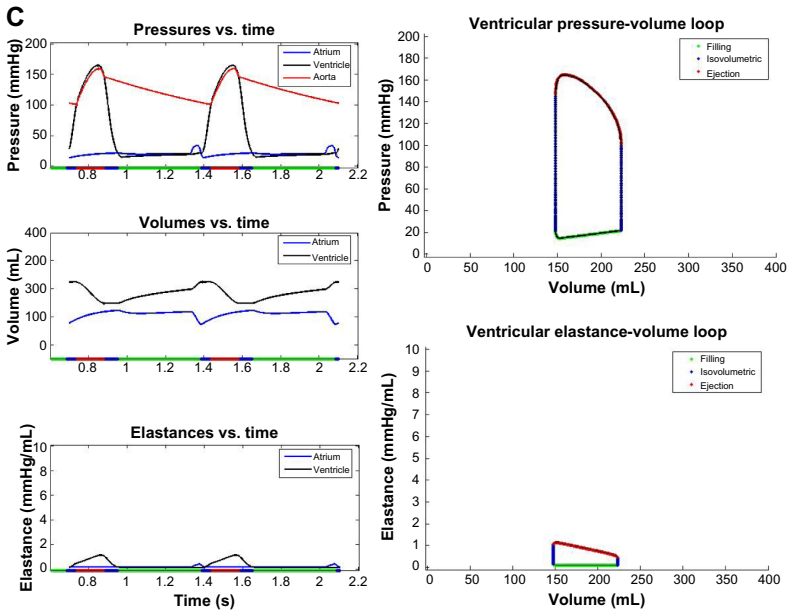

Figure 2. (**A**) The simulated pressures, volumes, and elastances for healthy control conditions. Left column: Pressures (top), volumes (middle), and elastances (bottom) as function of time with the colors as follows: atrium in blue, ventricle in black, and arterial in red. The colors of the abscissa refer to cardiac phases: filling in green, ejection in red, and both iso-volumetric phases in blue. Right column: Pressure–volume loop (top) and elastance–volume loop (bottom) with the colors referring to the cardiac phases: filling in green, ejection in red, and both iso-volumetric phases in blue. (**B**) Simulation for HFpEF conditions (see legend Fig. 2A). (**C**) Simulation for HFrEF conditions (see legend Fig. 2A).

Note that in Figure 6, the ventricular volume and ventricular EF (third row, third and fourth graph) are shown as a function of diastolic pressure in the aorta. The rationale for this exception is that end-diastolic pressure in the aorta (P_{DIAS}) was identified as one of the determinants of ESV but P_{DIAS} is a *variable* calculated in a simulation with the model while the other running variables are *parameters* set in the model. In order to vary P_{DIAS}, the parameter capillary resistance (R_C) was varied instead with the results plotted with P_{DIAS} on the abscissa.

In Figures 3–7, the graphs with ventricular volume versus the varying parameter (third row, third graph from left) show that the EDV and ESV vary in correspondence with Eqns. (5) and (6); ie, for EDV a proportional relation with filling pressure (P_{FILL}) and an inverse proportional relation with diastolic elastance (E_{MIN}) is found, and moreover, for ESV a proportional relation with diastolic pressure in the aorta (P_{DIAS}) and an inverse proportional relation with systolic elastance (E_{MAX}) is found. Finally, for both EDV and ESV a proportional relation with the zero-pressure ventricular volume (V_0) is found. These findings confirm Eqns. (5) and (6).

The ESV–EDV graphs in Figures 3–7 are found to be quite different. Table 2 summarizes the slopes and intercepts of these lines. Clearly, the same line is found by varying the diastolic elastance (E_{MIN}) and filling pressure (P_{FILL}), the major determinants of EDV (Eq. (5)), and also, another line is found by varying the systolic elastance (E_{MAX}) and diastolic pressure in the aorta (P_{DIAS}), the major determinants of ESV (Eq. (6)). Thus, because of the differences in slopes and intercepts of these lines in the ESV–EDV graph, it might be possible to infer the involvement of diastolic factors (filling pressure or diastolic elastance) or, in contrast, systolic factors (the diastolic pressure in the aorta or the systolic elastance) on the basis of the location of a patient's EDV and in ESV in the ESV–EDV graph.

Table 2. Numerical values of slopes and intercepts of the lines in the ESV–EDV graphs.

RUNNING VARIABLE	SLOPE	INTERCEPT
Diastolic elastance (E_{MIN})	0.26	16
Filling pressure (P_{FILL0})	0.26	16
Systolic elastance (E_{MAX})	2	–200
Diastolic pressure in aorta (P_{DIAS})	2.1	–200
Zero-pressure ventricular volume (V_0)	1	–73

The EF–ESV graphs in Figures 3–7 show that, although the graphs are rather different, the results (ie, lines) overlap in a common region of the graph. So, from the position of the line in the EF–ESV graphs, it cannot be interpreted which of the factors was involved. This is a disadvantage of the EF–ESV graph in comparison with the ESV–EDV graph.

Discussion

By using a simple mathematical model of a monoventricular cardiovascular system, this study identified the major determinants of EDV and ESV and, by the same token, the major

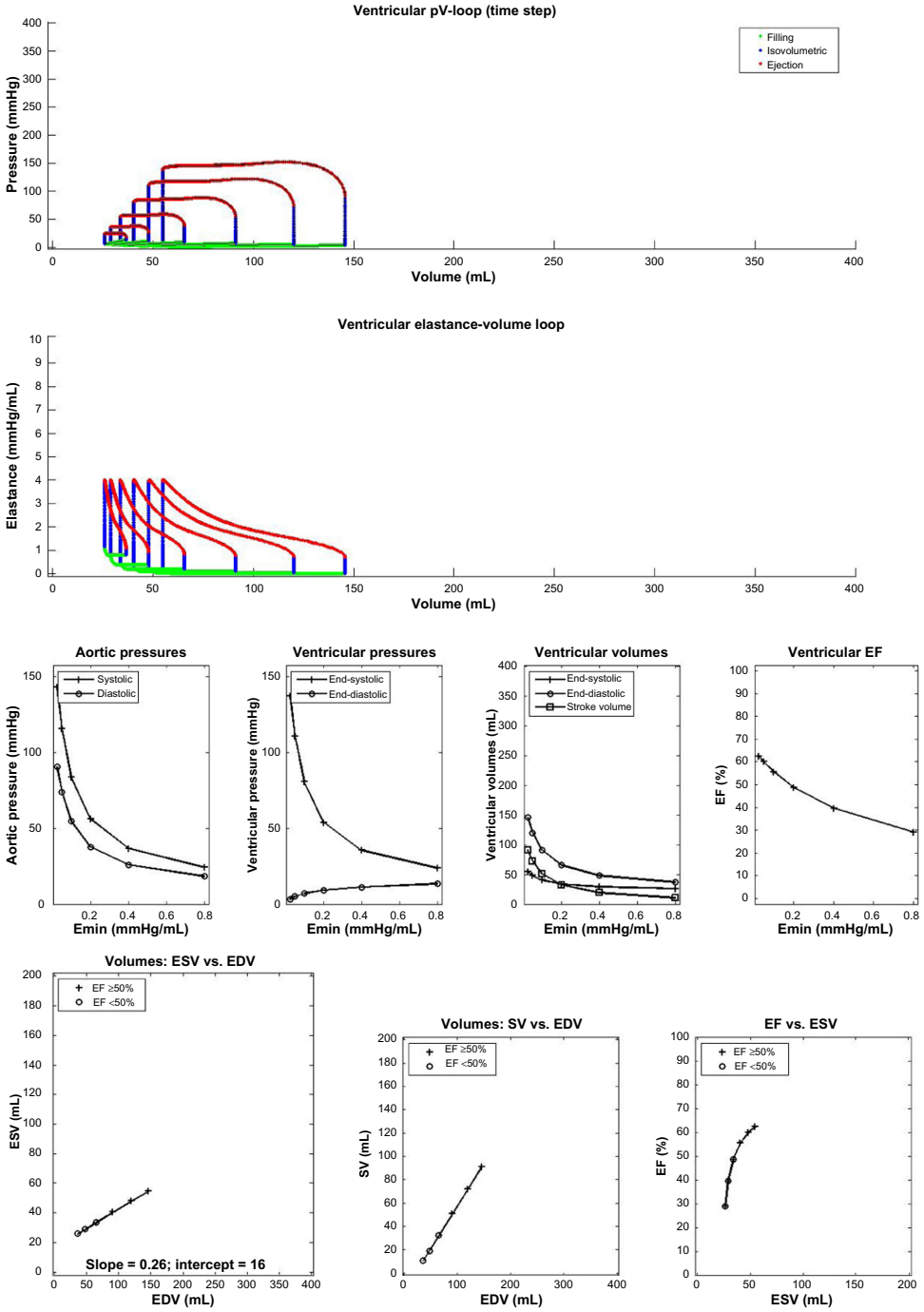

Figure 3. For control setting, simulation results for increasing diastolic elastance (E_{MIN}) of 0.025, 0.05, 0.1, 0.2, 0.4, and 0.8 mmHg/mL, respectively. First and second row show the left ventricular pressure–volume and elastance–volume loops, respectively. Third row shows the arterial and ventricular pressures and the ventricular volumes, SV, and EF are shown as functions of the diastolic elastance. Fourth row shows the ESV–EDV plot (with slope and intercept of regression line) and the Starling curve with SV as function of EDV.

determinants in the graph of ESV versus EDV and the EF, in particular, for the different phenotypes HFpEF and HFrEF.

By using Suga–Sagawa's elastance model of ventricular function (Eq. (3) and a simple mathematical reasoning (Eqns. (5) and (6)), the diastolic elastance and the filling pressure were identified as the major determinants of EDV, while the systolic elastance and the end-diastolic aortic pressure were identified as the major determinants of the ESV. Simulations with the cardiovascular model, indeed, clearly confirmed these findings on the major determinants of ESV and EDV (see Figs. 3–7). Elsewhere, Shoucri described theoretical aspects of the relationship between EF and E_{MAX} in HFpEF patients with emphasis on iso-volumic pressure (ie, the active force of the myocardium).[15]

Unfortunately, filling pressure and elastance during systole and diastole are difficult to measure in clinical practice.

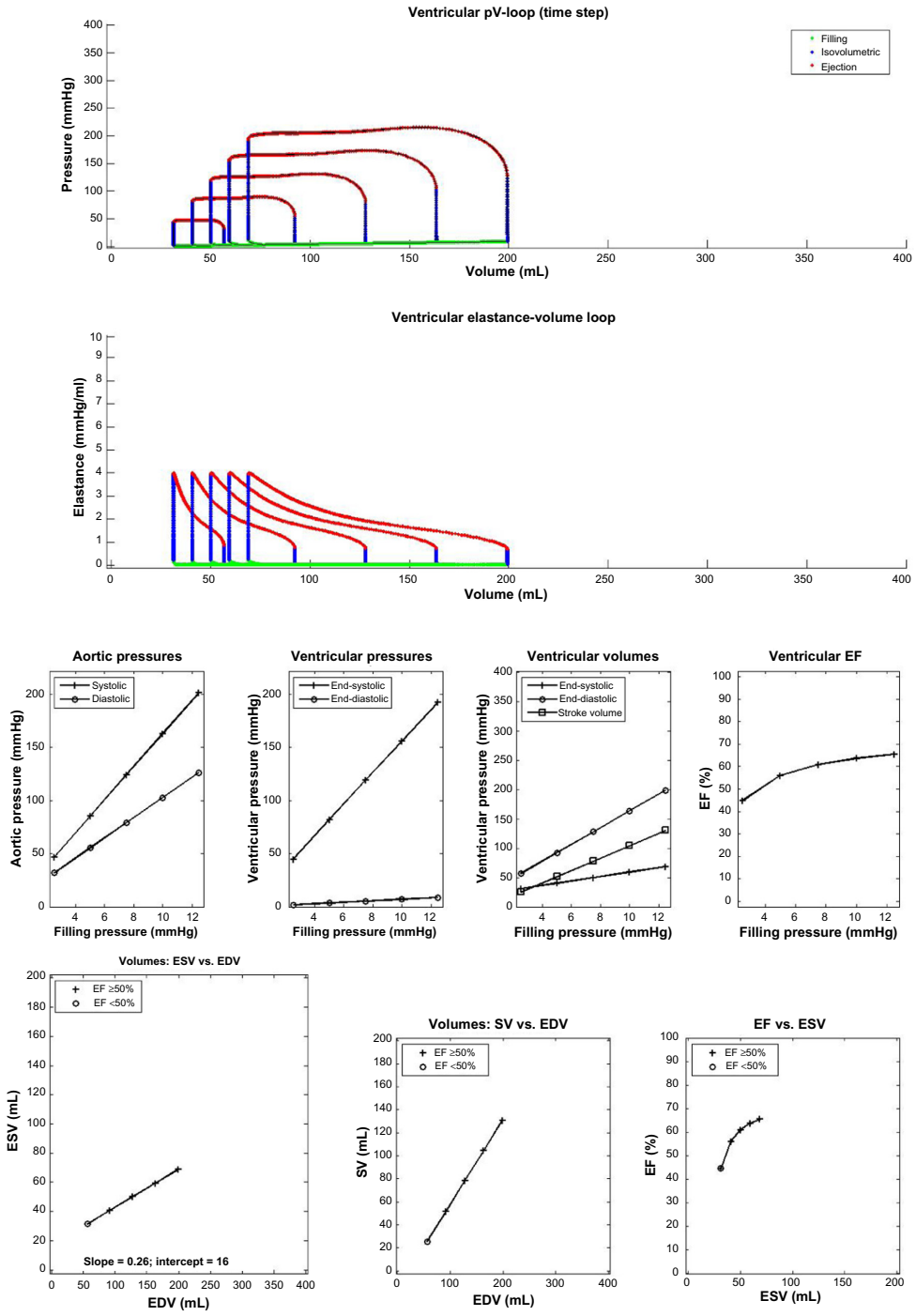

Figure 4. For control setting, simulation results for increasing filling pressures of 2.5, 5, 7.5, 10, and 12.5 mmHg, respectively. See legend of Figure 3 for further explanation.

But, in contrast, EDV and ESV are far more easily measured in standard clinical routine using modern imaging modalities. Thus, EDV and ESV can be regarded as measures that are closely related (Eqns. (5) and (6)) to the major determinants of the filling and diastolic pressures and the diastolic and systolic elastances. In fact, by virtue of our findings in Eqns. (5) and (6), the EDV is related to a normalized preload, ie, the filling pressure relative to the diastolic elastance (neglecting the zero-pressure ventricular volume V_0), while the ESV is related to as a normalized afterload, ie, the end-diastolic pressure in the aorta relative to the systolic elastance (neglecting the V_0). So, EDV and ESV represent, in a normalized form, the classical concepts, of preload and afterload, respectively.

In using ESV and EDV in clinically diagnostic decision making, a graph with the ESV on the ordinate and EDV on the abscissa (the so-called ESV–EDV graph) allows the representation of ESV and EDV independently, and, with that, the normalized preload and afterload. This study showed that

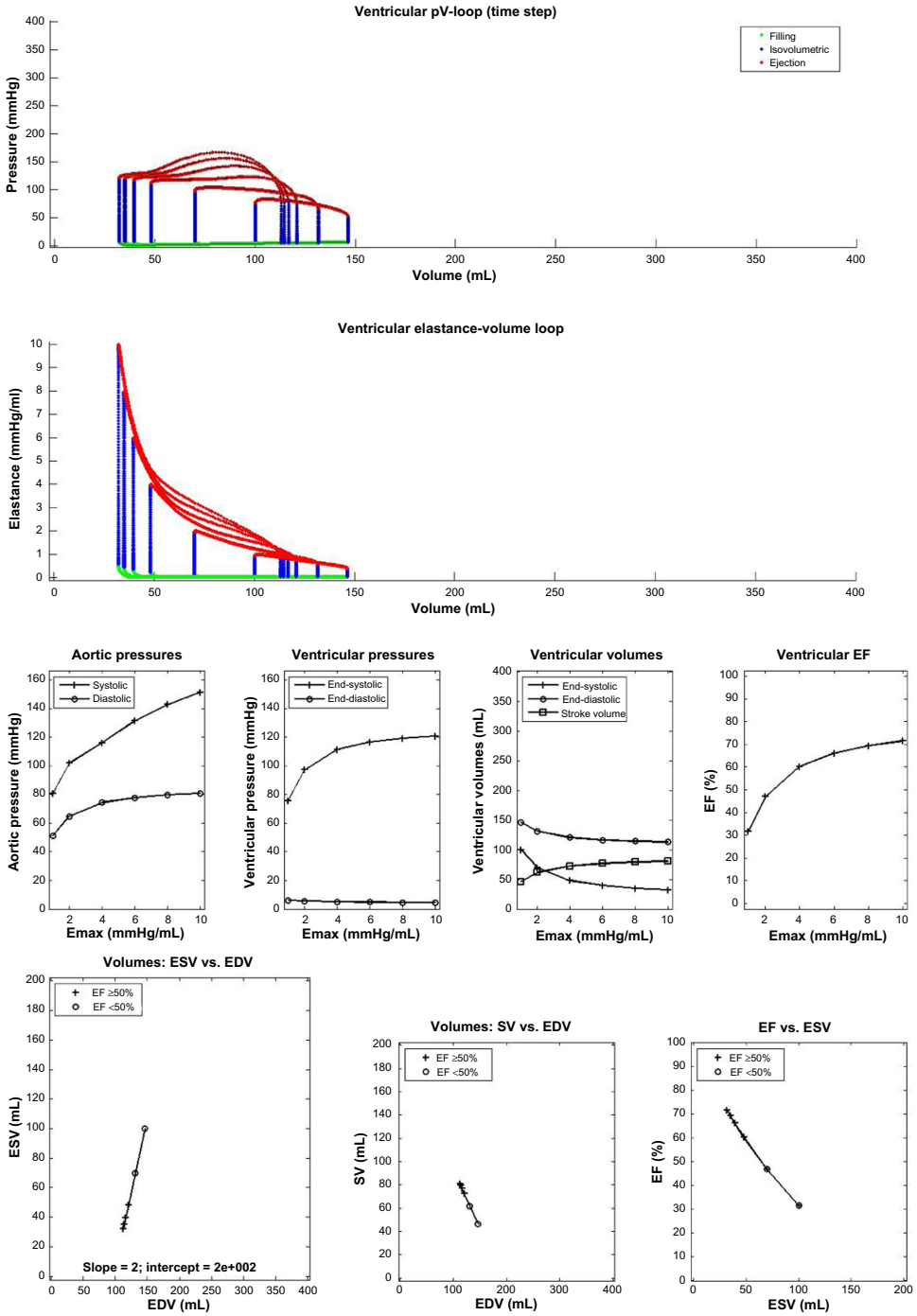

Figure 5. For control setting, simulation results for increasing systolic elastance (E_{MAX}) of 1, 2, 4, 6, 8, and 10 mmHg/mL, respectively. See legend of Figure 3 for further explanation.

the HFpEF and HFrEF are represented in this ESV–EDV graph with different regression lines and, moreover, that the slope of the regression lines is related to the EF (see Eq. (2) in Introduction). That is, the lower the EF, the steeper the regression line, although this relation is obscured considerably by the EDV. So, the ESV–EDV graph allows the differentiation between the phenotypes HFpEF and HFrEF (Fig. 1).

This differentiation of HFpEF and HFrEF in the ESV–EDV graph, on the basis of the ESV and EDV, can be given a more (patho-)physiological interpretation. Table 1 shows that the major difference between HFpEF and HFrEF as regards the maximum elastance (ie, the systolic elastance) is 7.98 mmHg/mL in HFpEF and 1.13 mmHg/mL in HFrEF, while in both groups the left ventricular end-diastolic pressure (LV EDP), as a measure of the filling pressure, is elevated to around 22.5 mmHg (much higher than 7 mmHg typically found in healthy controls) and, finally, the diastolic pressure in the aorta is 73 mmHg (around 70–80 mmHg typically found in

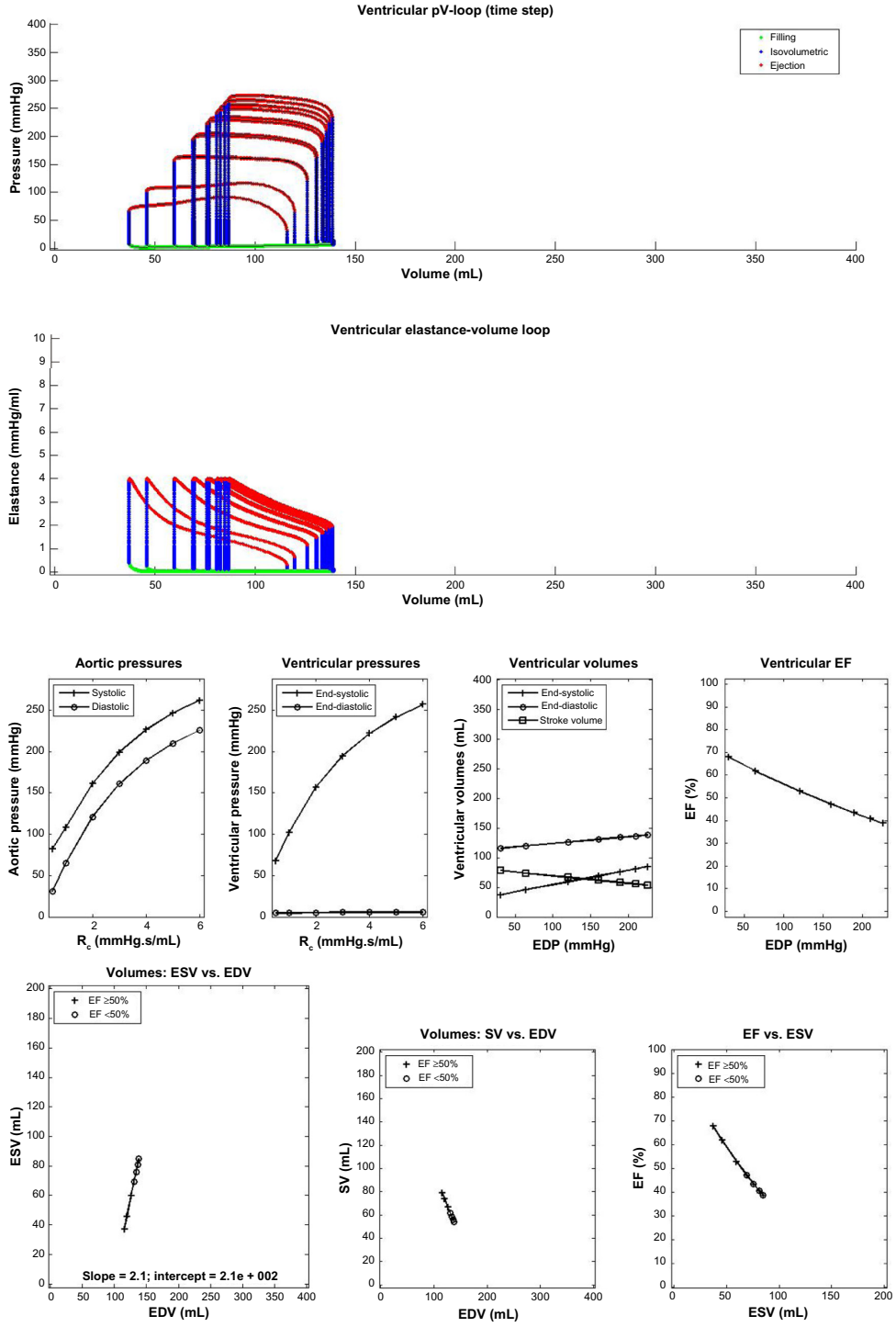

Figure 6. For control setting, simulation results for increasing capillary resistance (R_C) of 0.6, 1, 2, 3, 4, 5, 6 mmHg·s/mL, respectively. See legend of Figure 3 for further explanation. Note that the ventricular volume and ventricular EF (third row, third, and fourth graph are shown as function of end-diastolic pressure in the aorta).

healthy controls). This finding shows that the normalized afterload (end-diastolic pressure in the aorta relative to the systolic elastance) is significantly increased from 9.2 mL in HFpEF to 64 mL in HFrEF (from Table 1 by dividing diastolic pressure by E_{MAX}), a finding that is reflected by the ESV, ie, 27.66 mL in HFpEF and 147.02 mL in HFrEF (Table 1). Note that the ratios are almost equal, ie, 9.2/64 = 0.15 fairly well compares with 27.66/147.02 = 0.19. So, this confirms that the ESV may be given a (patho-)physiological interpretation as normalized afterload with end-diastolic aortic pressure and systolic elastance as major determinants. Likewise, the pathophysiological interpretation of the normalized preload (filling pressure relative to the diastolic elastance) could be confirmed by experimental findings. Unfortunately, Kerkhof et al.[8,16]

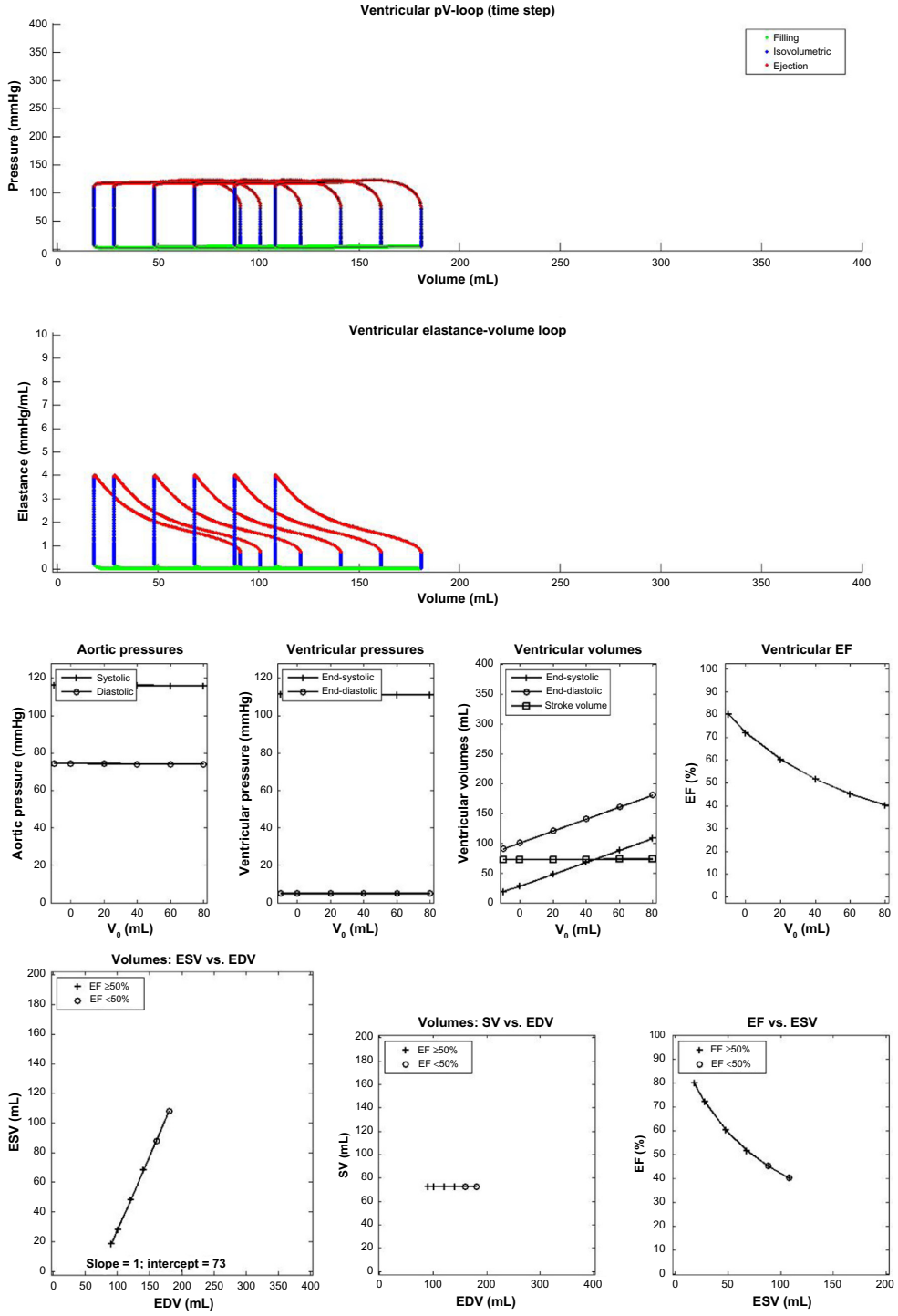

Figure 7. For control setting simulation results for increasing zero-pressure ventricular volume (V_0) of –10, 0, 20, 40, 60, 80 mL, respectively. See legend of Figure 3 for further explanation.

provided no data on the diastolic elastance. But, from the reported filling pressure of around 22.5 mmHg in both groups, considerably higher than in healthy controls, and the significantly increased EDV of 224.95 mL in HFrEF compared to 113.47 mL in HFpEF (Table 1), we calculate a diastolic elastance of 0.2 mmHg/mL in HRrEF and of 0.1 mmHg/mL in HFpEF (calculated from Table 1 by dividing LVEDP by EDV). For an equally increased filling pressure and a two-fold larger diastolic elastance, the normalized preload in HFrEF is expected to be twice as large as in HFpEF, a finding reflected by EDV in HFrEF and HFpEF. We infer that the EDV may be given a (patho-)physiological interpretation as normalized preload with filling pressure and diastolic elastance as major determinants. So, the ESV–EDV graph differentiates between HFpEF and HFrEF and, moreover, may be given a (patho-) physiological interpretation.

In contrast to the ESV–EDV graph that represents the ESV and EDV independently, the EF summarizes the ESV and EDV in one single metric and with that the EF summarized the complex interplay of cardiac filling and ejection in one metric. In terms of our model, the interplay of systolic and diastolic elastances as well as the filling and the end-diastolic aortic pressures, as the major determinants of ESV and EDV, are mapped into a single number with a size between 0 and 100%. Given the complex interplay of the major determinants (see Eq. (8)), it is highly implausible that each (patho-) physiological condition in one of the determinants is mapped into a unique numerical value of the EF and, consequently, it is equally implausible that a given value of the EF can be interpreted unambiguously in terms of the underlying (patho-) physiological mechanism. Loss of insight is the price paid for summarizing too briefly.

From these model-based results, one may infer that a plot of a patient's ESV and EDV in the ESV–EDV graph allows a clinical differentiation between diastolic or systolic involvement while the EF does not offer such a distinction. So, the ESV–EDV graph allows a better tool for the understanding of HFrEF and HFpEF. However, this model-based result is a guidance for future clinical research that should establish the practical value of the ESV–EDV graph over the single metric of EF.[1]

The advantage of mathematical modeling is the experimenter's full control of all parameters and conditions in the model and, with that, the simplicity to carry out a simulation experiment that is not so easily clinically performed. The validity of the modeling study needs, however, to be demonstrated by either the validity of model itself or by the validity of the obtained results. In this study, the validity of the model is based on the following considerations: (1) The model is built up of well-established components (ie, Suga–Sagawa's elastance model of the ventricle, Senzaki et al's normalized elastance function, and the generally accepted three-element Windkessel model of the arterial circulation).[17] (2) By comparing the simulation results (Fig. 3) with the pressure and volumes in HFpEF and HFrEF (Table 1), we recognize the validity of the model. (3) By using the Suga–Sagawa's elastance model, major determinants of the ESV and EDV were identified and these major determinants correspond with the simulations as well as the pathophysiological knowledge, ie, (a) diastolic elastance and filling pressure together mainly determine EDV, while (b) systolic elastance and end-diastolic pressure in the aorta together mainly determine ESV. In this perspective of the model's validity, we suggest to use our findings as a guidance in future clinical studies in order to provide supporting evidence.

Limitations

Although the model mimics the characteristics of control, HFpEF, and HFrEF patients quite accurately, this study clearly has its limitations because of the assumptions made in our mathematical model. To be more specific, (1) only the systemic part of the circulation is modeled with a mono-atrial–ventricular heart connected to a simple model of the filling system of the heart and a three-element Windkessel extended with a venous part, to model the systemic circulation. (2) The system is an open loop with the simple model of a filling system that is not connected to the venous part of systemic circulation. (3) The model represents a denervated heart and a circulation without many control mechanisms, eg, neuro-humoral control of heart rate, flow resistance, filling pressure, and cardiac contractility. For some of the limitations, we could compensate by choosing adequate parameters – eg, the different filling pressures, heart rate, maximum elastance in HFpEF and HFrEF – while other features will be incorporated in a future more advanced model – eg, a model with a closed circulation of both the systemic and the pulmonary circulation including neuro-humoral mechanisms. It is to be expected that a more advanced model will reveal more details in the determining factors of ESVs and EDVs (and with that in the ESV–EDV plots and EF). Nevertheless, it is hoped that the present insight will provide an adequate guidance for both clinical and modeling studies in the future.

Conclusion

By using a simple mathematical model of the circulation, the filling pressure and diastolic elastance are identified as the major determinants of EDV, while the end-diastolic aortic pressure in the aorta and the systolic elastance are identified as the major determinants of the ESV. By mathematical analysis and with simulations, the dependence of the EF and the ESV–EDV graph on the determinants was studied. It was found that the ESV–EDV graph allows the separation between diastolic and systolic dysfunction, while these two pathologies are intricately summarized in the single metric of EF. Therefore, the ESV–EDV graph can provide an advantage in HF studies.

Author Contributions

Conceived and designed the simulation experiments: TF, PK. Analyzed the data: TF, PK. Wrote the first draft of the manuscript: TF. Contributed to the writing of the manuscript: PK. Agree with manuscript results and conclusions: TF, PK. Jointly developed the structure and arguments for the paper: TF, PK. Made critical revisions and approved final version: TF, PK. Both authors reviewed and approved of the final manuscript.

REFERENCES

1. Kerkhof PL. Characterizing heart failure in the ventricular volume domain. *Clin Med Insights Cardiol*. 2015;9(suppl 1):11–31.
2. McMurray JJ, Adamopoulos S, Anker SD, et al; ESC Guidelines for the Diagnosis and Treatment. ESC guidelines for the diagnosis and treatment of acute and chronic heart failure 2012: the task force for the diagnosis and treatment of acute and chronic heart failure 2012 of the European Society of Cardiology. Developed in collaboration with the Heart Failure Association (HFA) of the ESC. *Eur Heart J*. 2012;33(14):1787–847.

3. Penicka M, Bartunek J, Trakalova H, et al. Heart failure with preserved ejection fraction in outpatients with unexplained dyspnea: a pressure-volume loop analysis. *J Am Coll Cardiol*. 2010;55:1701–10.
4. Hugenholtz PG, Wagner HR. Assessment of myocardial function in congenital heart disease. In: Adams FH, Swan HJ, Hall VE, eds. *Pathophysiology of Congenital Heart Diseases*. Berkeley: University California Press; 1970:201–30.
5. Robotham JL, Takata M, Berman M, Harasawa Y. Ejection fraction revisited. *Anesthesiology*. 1991;74:172–83.
6. Marmor A, Jain D, Zaret B. Beyond ejection fraction. *J Nucl Cardiol*. 1994;1: 477–86.
7. Manisty CH, Francis DP. Ejection fraction: a measure of desperation? *Heart*. 2008;94:400–1.
8. Kerkhof PL, Kresh JY, Li JK, Heyndrickx GR. Left ventricular volume regulation in heart failure with preserved ejection fraction. *Physiol Rep*. 2013;1:e00007.
9. Mann DL, Bogaev R, Buckberg GD. Cardiac remodelling and myocardial recovery: lost in translation? *Eur J Heart Fail*. 2010;12(8):789–96.
10. Beringer JY, Kerkhof PL. A unifying representation of ventricular volumetric indexes. *IEEE Trans BME*. 1998;45:365–71.
11. Suga H, Sagawa K, Shoukas AA. Load independence of the instantaneous pressure-volume ratio of the canine left ventricle and effects of epinephrine and heart rate on the ratio. *Circ Res*. 1973;32(2):314–22.
12. Senzaki H, Chen CH, Kass DA. Single-beat estimation of end-systolic pressure-volume relation in humans. A new method with the potential for noninvasive applications. *Circulation*. 1996;94(10):2497–506.
13. Suga H. Ventricular energetics. *Physiol Rev*. 1990;70:247–77.
14. Katz AM. *Physiology of the Heart*. Philadelphia: Lippincott William & Wilkins; 2006.
15. Shoucri RM. ESPVR, ejection fraction and heart failure. *Cardiovasc Eng*. 2010;10:207–12.
16. Kerkhof PL, Li JK, Heyndrickx GR. Effective arterial elastance and arterial complicance in heart failure patients with preserved ejection fraction. In: 35th Annual International Conference in the IEEE EMBS, Osaka, Japan, July 3–7, 2013.
17. Westerhof N, Stergiopulos N, Noble M. *Snapshots of Hemodynamics: An Aid for Clinical Research and Graduate Education*. New York: Springer; 2005. Physics of Heart & Circulation.

Appendix A. Mathematical Model of the Circulation

This mathematical model comprises one half of the circulation, implying that the pulmonary circulation referring to the right ventricle (RV) is not included as a separate entity. This limitation means that LV–RV interaction is not considered. Also, interaction with the pericardium is not covered. These restrictions are assumed to only minimally influence our results, particularly because the present study does not intend to simulate pathology of the RV or pericardium. Thus, we concentrate on the systemic circulation. Figure A1 shows the circuitry in terms of an electrical analog. To be specific, from left to right:

- The heart, filled from a constant pressure source P_{FILL0} through a fluid resistance R_{VS2AT}, consists of an atrium and a ventricle – which are both modeled with a time-varying elastance $E_{AT}(t)$ for the atrium and $E_{VL}(t)$ for the ventricle with time t as independent variable– and, moreover, the two valves each are represented by one-way diodes with valvular resistances R_{AT2VL} and R_{VL2AR} in series, where the resistors mimic the small flow resistance of the valves.
- The circulation consists of a three-element Windkessel model – a characteristic impedance Z_{AR0}, a total arterial compliance C_{AR}, a total vascular resistance R_C – and a venous part with a total venous compliance C_{VS}, and a total venous resistance R_{VS} connected to a constant pressure source P_{VS0}.

In this model, the standard symbols read as follows: (1) the rectangular elements represent Poiseuille fluid resistances (mmHg·s/mL), (2) the parallel lines represent both the volume storage capacity of compliant vessels (mL/mmHg), as well as (3) the time-varying elastances (mmHg/mL) of the atrium and ventricle, and, finally, (4) the circles represent constant pressure sources (mmHg). The connecting lines represent how the blood is flowing through the different components in the circulation.

Blood flow is defined for every branch in the circuitry by a pertinent name, eg, $F_{AT}(t)$. The flow is defined as positive in the direction of the arrow. Pressure is defined for almost every node in the analog by a specific name, eg, $P_{AT}(t)$; the pressure is measured relative to the bottom line of the analog (in electrical engineering terms relative to the "ground" as depicted by the symbol with the multiple parallel lines of unequal length at the bottom line).

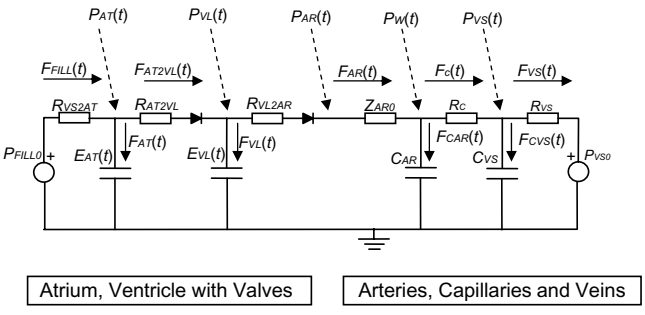

Figure A1. Electrical analog of the circulation (see text for discussion).

In the following calculations, we employ the standard mathematical–physical nomenclature ie, a single italic letter is used to refer to a variable or a parameter (like: V for volume, C for compliance), while one or more characters in a subscript are used to distinguish between different variables and parameters (such as C_{AT} and C_{VE}). Moreover, with t used as symbol for time, a time dependence of a variable is indicated by adding (t) to the right of the variable (eg, $V_{VL}(t)$ for a time-varying ventricular volume). The time derivative is, in Leibniz's notation, indicated as $dV_{VL}(t)/dt$. Finally, variables or parameters written in combination are to be interpreted as a multiplication (such as: $C_{VL}dP_{VL}(t)/dt$ for the multiplication of C_{VL} and $dP_{VL}(t)/dt$). The rationale of this nomenclature is an unambiguous and compact notation that facilitates easy calculus.

To simulate this model numerically by employing MATLAB, six steps need to be made. First, for each of the components of the analog, the constitutive relations need to be specified. Second, the state variables need to be chosen, where the governing rule is that one state variable is needed for every component with a derivative in its constitutive relation. Third, the conditions governing the opening and closing of the valves need to be reformulated in terms of the state variables. Note that there are four combinations for the two valves system: closed-closed (iso-volumetric phase), open-closed (filling phase), closed-open (ejecting phase), and open-open (remaining phase). Fourth, a state equation for each of the four state variables is calculated from the analog and the constitutive relations, but each cardiac phase requires its own equation. Thus, for each of the four cardiac phases, four state equations are calculated. Fifth, the analog and the constitutive relations are used to formulate auxiliary equations that enable the calculation of other variables of interest from the state variables. Sixth, the state and auxiliary equations need to be programmed and tested in a suitable software development environment, like MATLAB. In the following, for reasons of brevity, the last two steps are discussed in less detail. The full approach will be described as five consecutive stages.

I. To start with, the following constitutive relations are defined in the analog:

For every node, the local flows add to zero, taking the direction of the flows into account. For example, at the node with pressure $P_{AT}(t)$, the relation $F_{FILL}(t) - F_{AT}(t) - F_{AT2VL}(t) = 0$ holds.

In every branch containing a single Poiseuille resistor, the flow equals the pressure difference divided by the resistance. For example, for the branch with flow $F_{FILL}(t)$, the relation $F_{FILL}(t) = (P_{FILL0}(t) - P_{AT}(t))/R_{VS2AT}$ holds. Note that the one-way flow characteristic of a valve (diode) complicates the relation between pressure difference, flow, and resistance. That is, if the pressure on the left side of the valve is smaller

than the pressure at the right, then the valve is closed. For example, for the uttermost left branch with a valve, the following relations holds: (1) if $P_{AT}(t) < P_{VL}(t)$ (ie, valve closed), then $F_{AT2VL}(t) = 0$ and, conversely, (2) if $P_{AT}(t) \geq P_{VL}(t)$ (ie, valve open), then the relation $F_{AT2VL}(t) = (P_{AT}(t) - P_{VL}(t))/R_{AT2VL}$ holds. Therefore, the valve is in fact described by two relationships that have to be dealt with.

In every branch with a compliant vessel, the flow equals the vessel's rate of volume change and, this in turn, equals the compliance times the rate of pressure change. For example, for the compliance C_{AR}, the relation $F_{AR} = dV_{AR}(t)/dt = C_{AR}dP_W(t)/dt$ holds.

Finally, in the branches including the atrium and the ventricle, the flow equals the rate of volume chance. For the ventricle, for example, $F_{VL}(t) = dV_{LV}(t)/dt$. The pressure–volume relation is given by the time-varying elastance model of Suga and Sagawa.[11] For the ventricle, for example, the relation $P_{VL}(t) = E_{VL}(t)\{V_{VL}(t) - V_{VL0}\}$ holds. The time-varying elastance of the ventricle $E_{VL}(t)$ is defined by a modification of Senzaki et al's elastance function.[12] For the iso-volumetric and ejecting phases, Senzaki et al's elastance function is scaled in amplitude so that it fits between a predefined maximum and minimum elastance; for the filling and remaining phases of the ventricle, the elastance is equal to the minimum elastance. Finally, the elastances are scaled in time so that they fit in predefined filling and nonfilling parts of the cardiac cycle.

This completes the description of the constitutive relations.

II. The following state variables are selected: the atrial volume $V_{AT}(t)$, the ventricular volume $V_{VL}(t)$, the Windkessel pressure $P_W(t)$, and the venous pressures $P_{VS}(t)$. This selection comprises all components with a derivative in its constitutive relation and, thus, defines the set of the state variables.

III. The conditions that govern the opening and closing of the valves need to be reformulated in terms of the state variables. That is, the pressures $P_{AT}(t)$, $P_{VL}(t)$, and $P_{AR}(t)$ need to be reformulated in terms of the four state variables $V_{AT}(t)$, $V_{VL}(t)$, $P_W(t)$, and $P_{VS}(t)$.

The volume–pressure relations for the atrium and ventricle, as given by the Suga–Sagawa model, allow the direct calculation of the required pressure $P_{AT}(t)$ and $P_{VL}(t)$ from the state variables $V_{AT}(t)$ and $V_{VL}(t)$. So, $P_{AT}(t)$ and $P_{VL}(t)$ follow directly from $V_{AT}(t)$ and $V_{VL}(t)$ using the Suga–Sagawa relation.

A somewhat more sophisticated reasoning is required to calculate the pressure $P_{AR}(t)$ in terms of the state variables $P_{AT}(t)$, $P_{VL}(t)$, $P_W(t)$, and $P_{VS}(t)$. If the valve is closed (iso-volumetric and filling phase), then the flow $F_{AR}(t)$ is zero and, consequently, the pressure drop over Z_{AR0} is zero and, hence, $P_{AR}(t)$ equals $P_W(t)$. Thus, for a closed valve, the condition $P_{VL}(t) < P_{AR}(t)$ can be rewritten as $P_{VL}(t) < P_W(t)$. In the opposite case of an open valve (ejecting and remaining phase), the resistors $R_{VL2\,AR}$ and Z_{AR0} form a series connection with a pressure difference $P_{VL}(t) - P_W(t)$ applied. Hence, $P_{AR} = P_W + \alpha(P_{VL} - P_W) = (1-\alpha)P_W + \alpha P_{VL}$, with $\alpha = Z_{AR0}/(R_{VL2\,AR} + Z_{AR0})$ and, hence, the auxiliary variable P_{AR} can be calculated directly from the state variables $P_W(t)$ and $P_{VL}(t)$. The condition $P_{VL} < P_{AR}$ can now be written as $P_{VL} < P_{AR} = (1-\alpha)P_W + \alpha P_{VL}$ and this result can be rewritten, by subtraction of αP_{VL}, as $(1-\alpha)P_{VL} < (1-\alpha)P_W$, which can be further simplified to $P_{VL} < P_W$ by dividing by $(1-\alpha)$ (provided that $1 - \alpha \neq 0$, implying that $R_{VL2\,AR} \neq 0$). Again, the condition $P_{VL}(t) < P_{AR}(t)$ can be rewritten as $P_{VL}(t) < P_W(t)$. In conclusion, the condition $P_{VL}(t) < P_{AR}(t)$ is equivalent to the conditions $P_{VL}(t) < P_W(t)$. And, conversely, the condition $P_{VL}(t) \geq P_{AR}(t)$ is equivalent to the conditions $P_{VL}(t) \geq P_W(t)$.

With this result, the four conditions that determine the four cardiac phases, can be written in term of the state variables. To be specific:

- In the *iso-volumetric* phase (with both valves closed), the ventricular pressure $P_{VL}(t)$ is larger than the atrial pressure $P_{AT}(t)$ and, at the same time, smaller than the arterial pressure $P_{AR}(t)$, ie, $P_{AT}(t) < P_{VL}(t)$ and $P_{VL}(t) < P_{AR}(t)$. This is rewritten in terms of the state variables as $P_{AT}(t) < P_{VL}(t)$ and $P_{VL}(t) < P_W(t)$.
- In the *ejection-phase* (with a closed valve between the atrium and ventricle and, moreover, an open valve between ventricle and arterial circulation), the ventricular pressure $P_{VL}(t)$ is larger than the atrial pressure $P_{AT}(t)$ and, at the same time, larger than or equal to the arterial pressure $P_{AR}(t)$, ie, $P_{AT}(t) < P_{VL}(t)$ and $P_{VL}(t) \geq P_{AR}(t)$. This is rewritten in terms of the state variables as $P_{AT}(t) < P_{VL}(t)$ and $P_{VL}(t) \geq P_W(t)$.
- In the *filling-phase* (with an open valve between the atrium and ventricle and, moreover, a closed valve between ventricle and arterial circulation), the ventricular pressure $P_{VL}(t)$ is smaller than or equal to the atrial pressure $P_{AT}(t)$ and, at the same time, smaller than the arterial pressure $P_{AR}(t)$, ie, $P_{AT}(t) \geq P_{VL}(t)$ and $P_{VL}(t) < P_{AR}(t)$. This is rewritten in terms of the state variables as $P_{AT}(t) \geq P_{VL}(t)$ and $P_{VL}(t) < P_W(t)$.
- Finally, in the *remaining phase* (with both valves open and assuming $P_{FILL0} \geq P_{VS0}$), that occurs some time after the heart completely stops beating (ie, death), the ventricular pressure $P_{VL}(t)$ is smaller or equal to the atrial pressure $P_{AT}(t)$ and is, at the same time, greater or equal than to the arterial pressure $P_{AR}(t)$, ie, $P_{AT}(t) \geq P_{VL}(t)$ and $P_{VL}(t) \geq P_{AR}(t)$. This is rewritten in terms of the state variables as $P_{AT}(t) \geq P_{VL}(t)$ and $P_{VL}(t) \geq P_W(t)$. Note that, this remaining phase is included for reasons of computational completeness but is not occurring during the simulations.

IV. From the analog model, for each of the four cardiac phases, a set of four differential equations (one equation for each state variable) is calculated.

However, the calculation starts, for all cardiac phases, with the Suga–Sagawa's pressure–volume relations which relate the atrial volume $V_{AT}(t)$ to the atrial pressure $P_{AT}(t)$ and, likewise, the ventricular volume $V_{VL}(t)$ to the ventricular pressure $P_{VL}(t)$ by the relations

$$\begin{aligned} P_{AT}(t) &= E_{AT}(t)\{V_{AT}(t) - V_{AT0}\} \\ P_{VL}(t) &= E_{VL}(t)\{V_{VL}(t) - V_{VL0}\} \end{aligned} \tag{9}$$

with the elastances $E_{AT}(t)$ and $E_{VL}(t)$ as defined by Senzaki et al.[12]

For the LV, Senzaki et al provide a formulation for the normalized elastance as a function of time, in terms of a Fourier series. Senzaki et al applied a double normalization such that the maximum of the amplitude equals 1 and that the normalized time moment of the maximum amplitude is also assigned to the value of 1.[12] In our model, we rescale Senzaki et al's normalized elastance in such a way that: (1) the duration of systole and diastole become equal to preset values of T_{SYS} and T_{DIA} and, moreover, (2) the elastances are shifted in such a way that the systolic part of the atrial elastance preceeds the systolic part of the ventrical elastance and, finally, (3) that the amplitude of the rescaled elastance is between the preset values of E_{MAX} for the maximum and E_{MIN} for the minimum. This adjusted elastance is employed for both the atrium and the ventricle, although differently scaled in amplitude and time. See Figure 2(A) (lower-left graph) for a clear example.

The Suga–Sagawa relation together with the Senzaki-elastance allow the calculation of the pressures. To be specific: for a given moment, first, the elastance is calculated using the Senzaki et al's elastance function and, then, the pressure is calculated from the elastance and the volume using Suga–Sagawa's relation. The calculation of the volume is discussed below.

In the ventricular *iso-volumetric phase*, both valves are closed with the conditions $P_{AT}(t) < P_{VL}(t)$ and $P_{VL}(t) < P_W(t)$. The state equation for the state variable atrial volume $V_{AT}(t)$ is found as follows:

$$\begin{aligned} F_{AT}(t) &= F_{FILL}(t) - F_{AT2VL}(t), \text{ with } F_{AT2VL}(t) = 0 \\ &\Rightarrow \frac{dV_{AT}(t)}{dt} = \frac{P_{FILL0}(t) - P_{AT}(t)}{R_{VS2AT}} \Rightarrow \\ &\boxed{\frac{dV_{AT}(t)}{dt} + \frac{1}{R_{VS2AT}} P_{AT}(t) = \frac{1}{R_{VS2AT}} P_{FILL0}(t)} \end{aligned} \tag{10}$$

A similar reasoning yields the state equation for ventricular volume $V_{LV}(t)$. That is:

$$\begin{aligned} F_{VL}(t) &= F_{AT2VL}(t) - F_{AR}(t), \text{ with } F_{AT2VL}(t) \\ &= F_{AR}(t) = 0 \Rightarrow F_{VL}(t) = \frac{dV_{VL}(t)}{dt} = 0 \\ &\boxed{\frac{dV_{VL}(t)}{dt} = 0} \end{aligned} \tag{11}$$

Note that, $dV_{LV}(t)/dt = 0$, implies that $V_{LV}(t)$ is constant as expected in the iso-volumetric phase.

Likewise, the state equation for the Windkessel pressure $P_W(t)$ is found:

$$\begin{aligned} F_{CAR}(t) &= F_{AR}(t) - F_C(t), \text{ with } F_{AR}(t) = 0 \\ &\Rightarrow C_{AR} \frac{dP_W(t)}{dt} = -\frac{P_W(t) - P_{VS}(t)}{R_C} \Rightarrow \\ &\boxed{C_{AR} \frac{dP_W(t)}{dt} + \frac{1}{R_C} P_W(t) = \frac{1}{R_C} P_{VS}(t)} \end{aligned} \tag{12}$$

Finally, the state equation for the venous pressure $P_{VS}(t)$ is found:

$$\begin{aligned} F_{CVS} &= F_C(t) - F_{VS}(t) \Rightarrow C_{VS} \frac{dP_{VS}(t)}{dt} \\ &= \frac{P_W(t) - P_{VS}(t)}{R_C} - \frac{P_{VS}(t) - P_{VS0}(t)}{R_{VS}} \Rightarrow \\ &\boxed{C_{VS} \frac{dP_{VS}(t)}{dt} + \left(\frac{1}{R_C} + \frac{1}{R_{VS}}\right) P_{VS}(t) = \frac{1}{R_C} P_W(t) + \frac{1}{R_{VS}} P_{VS0}(t)} \end{aligned} \tag{13}$$

In the ventricular *ejection phase* the atrial–ventricular valve is closed with condition $P_{AT}(t) < P_{VL}(t)$ and the ventricular–arterial valve is open with condition $P_{VL}(t) \geq P_W(t)$.

The state equation for the atrial volume $V_{AT}(t)$ equals the state equation in the iso-volumetric phase, ie, Eq. (10).

The state equation for the ventricular volume $V_{LV}(t)$ is:

$$\begin{aligned} F_{VL}(t) &= F_{AT2VL}(t) - F_{AR}(t), \text{ with } F_{AT2VL}(t) = 0 \\ &\Rightarrow \frac{dV_{VL}(t)}{dt} = -\frac{P_{VL}(t) - P_W(t)}{R_{VL2AR} + Z_{AR0}} \Rightarrow \\ &\boxed{\frac{dV_{VL}(t)}{dt} + \frac{1}{R_{VL2AR} + Z_{AR0}} P_{VL}(t) = \frac{1}{R_{VL2AR} + Z_{AR0}} P_W(t)} \end{aligned} \tag{14}$$

The state equation for the Windkessel pressure $P_W(t)$ is:

$$\begin{aligned} F_{CAR}(t) &= F_{AR}(t) - F_C(t) \Rightarrow C_{AR} \frac{dP_W(t)}{dt} \\ &= \frac{P_{VL}(t) - P_W(t)}{R_{VL2AR} + Z_{AR0}} - \frac{P_W(t) - P_{VS}(t)}{R_C} \Rightarrow \\ &\boxed{\begin{aligned} C_{AR} \frac{dP_W(t)}{dt} &+ \left(\frac{1}{R_{VL2AR} + Z_{AR0}} + \frac{1}{R_C}\right) P_W(t) \\ &= \frac{1}{R_{VL2AR} + Z_{AR0}} P_{VL}(t) + \frac{1}{R_C} P_{VS}(t) \end{aligned}} \end{aligned} \tag{15}$$

The state equation for the venous pressure $P_{VS}(t)$ takes the same form as the state equations for the iso-volumetric phase, ie, Eq. (13).

In the ventricular *filling phase*, the atrial–ventricular valve is open with condition $P_{AT}(t) \geq P_{VL}(t)$ and the ventricular–arterial valve is closed $P_{VL}(t) < P_W(t)$.

Table A.1. The Suga–Sagawa pressure–volume relations for the atrium and ventricle and the state equations for the four state variables ($V_{AT}(t)$, $V_{VL}(t)$, $P_W(t)$, and $P_{VS}(t)$) for each of the four cardiac phases.

% Atrial and ventricular pressure-volume relations:

$$P_{AT}(t) = E_{AT}(t)\{V_{AT}(t) - V_{AT0}\}$$
$$P_{VL}(t) = E_{VL}(t)\{V_{VL}(t) - V_{VL0}\}$$

if $P_{AT}(t) < P_{VL}(t)$ and $P_{VL}(t) < P_W(t)$ % Iso-volumetric phase

$$\frac{dV_{AT}(t)}{dt} = \frac{1}{R_{VS2AT}} P_{FILL0}(t) - \frac{1}{R_{VS2AT}} P_{AT}(t)$$
$$\frac{dV_{VL}(t)}{dt} = 0$$
$$C_{AR}\frac{dP_W(t)}{dt} = -\frac{1}{R_C} P_W(t) + \frac{1}{R_C} P_{VS}(t)$$
$$C_{VS}\frac{dP_{VS}(t)}{dt} = \frac{1}{R_C} P_W(t) - \left(\frac{1}{R_C} + \frac{1}{R_{VS}}\right) P_{VS}(t) + \frac{1}{R_{VS}} P_{VS0}(t)$$

if $P_{AT}(t) < P_{VL}(t)$ and $P_{VL}(t) \geq P_W(t)$ % Ejection phase

$$\frac{dV_{AT}(t)}{dt} = \frac{1}{R_{VS2AT}} P_{FILL0}(t) - \frac{1}{R_{VS2AT}} P_{AT}(t)$$
$$\frac{dV_{VL}(t)}{dt} = -\frac{1}{R_{VL2AR} + Z_{AR0}} P_{VL}(t) + \frac{1}{R_{VL2AR} + Z_{AR0}} P_W(t)$$
$$C_{AR}\frac{dP_W(t)}{dt} = \frac{1}{R_{VL2AR} + Z_{AR0}} P_{VL}(t) - \left(\frac{1}{R_{VL2AR} + Z_{AR0}} + \frac{1}{R_C}\right) P_W(t) + \frac{1}{R_C} P_{VS}(t)$$
$$C_{VS}\frac{dP_{VS}(t)}{dt} = \frac{1}{R_C} P_W(t) - \left(\frac{1}{R_C} + \frac{1}{R_{VS}}\right) P_{VS}(t) + \frac{1}{R_{VS}} P_{VS0}(t)$$

if $P_{AT}(t) \geq P_{VL}(t)$ and $P_{VL}(t) < P_W(t)$ % Filling phase

$$\frac{dV_{AT}(t)}{dt} = \frac{1}{R_{VS2AT}} P_{FILL0}(t) - \left(\frac{1}{R_{VS2AT}} + \frac{1}{R_{AT2VL}}\right) P_{AT}(t) + \frac{1}{R_{AT2VL}} P_{VL}(t)$$
$$\frac{dV_{VL}(t)}{dt} = \frac{1}{R_{AT2VL}} P_{AT}(t) - \frac{1}{R_{AT2VL}} P_{VL}(t)$$
$$C_{AR}\frac{dP_W(t)}{dt} = -\frac{1}{R_C} P_W(t) + \frac{1}{R_C} P_{VS}(t)$$
$$C_{VS}\frac{dP_{VS}(t)}{dt} = \frac{1}{R_C} P_W(t) - \left(\frac{1}{R_C} + \frac{1}{R_{VS}}\right) P_{VS}(t) + \frac{1}{R_{VS}} P_{VS0}(t)$$

if $P_{AT}(t) \geq P_{VL}(t)$ and $P_{VL}(t) \geq P_W(t)$ % Remaining phase

$$\frac{dV_{AT}(t)}{dt} = \frac{1}{R_{VS2AT}} P_{FILL0}(t) - \left(\frac{1}{R_{VS2AT}} + \frac{1}{R_{AT2VL}}\right) P_{AT}(t) + \frac{1}{R_{AT2VL}} P_{VL}(t)$$
$$\frac{dV_{VL}(t)}{dt} = \frac{1}{R_{AT2VL}} P_{AT}(t) - \left(\frac{1}{R_{AT2VL}} + \frac{1}{R_{VL2AR} + Z_{AR0}}\right) P_{VL}(t) + \frac{1}{R_{VL2AR} + Z_{AR0}} P_W(t)$$
$$C_{AR}\frac{dP_W(t)}{dt} = \frac{1}{R_{VL2AR} + Z_{AR0}} P_{VL}(t) - \left(\frac{1}{R_{VL2AR} + Z_{AR0}} + \frac{1}{R_C}\right) P_W(t) + \frac{1}{R_C} P_{VS}(t)$$
$$C_{VS}\frac{dP_{VS}(t)}{dt} = \frac{1}{R_C} P_W(t) - \left(\frac{1}{R_C} + \frac{1}{R_{VS}}\right) P_{VS}(t) + \frac{1}{R_{VS}} P_{VS0}(t)$$

Table A2. Numerical values of the model parameters for the cases of normal control, HFpEF, and HFrEF.

PARAMETER	CONTROL	HFpEF	HFrEF
C_{AR} (mL/mmHg)	1.50	0.94	1.30
C_{VS} (mL/mmHg)	15.0	9.40	13.0
Heart rate (bpm)	60.00	67.15	86.67
P_{FILL0} (mmHg)	7.0	22.9	22.2
P_{VS0} (mmHg)	8.0	23.9	23.2
R_{VS2AT} (mmHg·s/mL)	0.02	0.02	0.02
R_{AT2VL} (mmHg·s/mL)	0.02	0.02	0.02
R_{VL2AR} (mmHg·s/mL)	0.01	0.01	0.01
Z_{AR0} (mmHg·s/mL)	0.03	0.03	0.03
Atrium (Suga–Sagawa–Senzaki et al)			
E_{MIN} (mL/mmHg)	0.17	0.17	0.17
E_{MAX} (mL/mmHg)	0.9	0.32	0.4
V_0 (mL)	–2.7	–2.7	–2.7
Ventricle (Suga–Sagawa–Senzaki et al)			
E_{MIN} (mL/mmHg)	0.05	0.24	0.1
E_{MAX} (mL/mmHg)	4	8	1.13
V_0 (mL)	8	8	20

The state equation for the atrial volume $V_{AT}(t)$ is

$$\begin{aligned} F_{AT}(t) = F_{FILL}(t) - F_{AT2VL}(t) \Rightarrow \frac{dV_{AT}(t)}{dt} \\ = \frac{P_{FILL0}(t) - P_{AT}(t)}{R_{VS2AT}} - \frac{P_{AT}(t) - P_{VL}(t)}{R_{AT2VL}} \Rightarrow \\ \boxed{\frac{dV_{AT}(t)}{dt} + \left(\frac{1}{R_{VS2AT}} + \frac{1}{R_{AT2VL}}\right) P_{AT}(t) \\ = \frac{1}{R_{VS2AT}} P_{FILL0}(t) + \frac{1}{R_{AT2VL}} P_{VL}(t)} \end{aligned} \tag{16}$$

The state equation for the ventricular volume $V_{LV}(t)$ is

$$\begin{aligned} F_{VL}(t) = F_{AT2VL}(t) - F_{AR}(t), \text{ with } F_{AR}(t) = 0 \\ \Rightarrow \frac{dV_{VL}(t)}{dt} = \frac{P_{AT}(t) - P_{VL}(t)}{R_{AT2VL}} \Rightarrow \\ \boxed{\frac{dV_{VL}(t)}{dt} + \frac{1}{R_{AT2VL}} P_{VL}(t) = \frac{1}{R_{AT2VL}} P_{AT}(t)} \end{aligned} \tag{17}$$

The state equations for the pressures $P_W(t)$ and $P_{VS}(t)$ in the filling phase take the same form as the state equation in the iso-volumetric phase, ie, Eqns. (12) and (13).

In *remaining phase*, both valves open with conditions $P_{AT}(t) \geq P_{VL}(t)$ and $P_{VL}(t) \geq P_W(t)$.

The state equation for the atrial volume $V_{AT}(t)$ takes the same form as in the filling phase Eq. (16).

The state equation for the ventricular volume $V_{LV}(t)$ is:

$$\begin{aligned} F_{VL}(t) = F_{AT2VL}(t) - F_{AR}(t) \Rightarrow \frac{dV_{VL}(t)}{dt} \\ = \frac{P_{AT}(t) - P_{VL}(t)}{R_{AT2VL}} - \frac{P_{VL}(t) - P_W(t)}{R_{VL2AR} + Z_{AR0}} \Rightarrow \\ \boxed{\frac{dV_{VL}(t)}{dt} + \left(\frac{1}{R_{AT2VL}} + \frac{1}{R_{VL2AR} + Z_{AR0}}\right) P_{VL}(t) \\ = \frac{1}{R_{AT2VL}} P_{AT}(t) + \frac{1}{R_{VL2AR} + Z_{AR0}} P_W(t)} \end{aligned} \tag{18}$$

The state equations for state variables $P_W(t)$ and $P_{VS}(t)$ take the form of the ejecting phase and the iso-volumetric phase, respectively, ie, Eqns. (15) and (13).

This completes the state equations in each of the four distinct cardiac phases. All the state equations are summarized in Table A.1 while the typical values of the parameters are summarized in Table A2.

In fact, Table A1 can be considered as the model's equations in a pseudo-code. Then, an outline of the computational scheme to simulate the model is as follows: A built-in Matlab solver of differential equations calls the function with the state equations in Table A.1 and with the initial conditions of the four state variables and the time moment as input to the function. As a result, the function returns the derivatives of the four state equations to the solver. Then, the solver calculates the state variables at an incremental time moment from the initial conditions and these calculated derivatives. Next, the solver calls the function again but with the new values of the state variables and, as result, the new

derivatives of the state variables are returned. This process is repeated, again and again, until the end of the simulations interval is reached. The calculated values of the state variables at all time moments form the simulation result.

In order to ensure the nonnegativity of the state variables in the numerical calculations, the following rule was added. If a state variable was smaller than or equal to zero and the calculated derivative of the state variable was also smaller than zero at any particular instant, then the state variable's derivative was set equal to zero for that time moment. So, by this rule, a nonpositive value is not allowed to decrease. In the practice of small incremental time steps, this rule is sufficient to guarantee nonnegativity of the state variables.

All simulations started from the following initial conditions for the state variables:

V_{AT} = 10 mL, V_{VL} = 80 mL, P_W = 80 mmHg, P_{VS} = 10 mmHg. Each simulation run included a sufficient number of heart beats to guarantee a steady state in the simulation results. Results of the last beat were used in further analysis.

V. The calculated state variables allow the calculations of all other variables. To be specific: The atrial and ventricular pressures, $P_{AT}(t)$ and $P_{VL}(t)$, can be calculated from the atrial and ventricular volumes, $V_{AT}(t)$ and $V_{VL}(t)$, with the Suga–Sagawa relation for each time moment. Next, with this pressure and the state variables $P_W(t)$ and $P_{VS}(t)$, the flows in all the resistances can be calculated by Poiseuille's law, taking into account the characteristics of the valves. For example: (1) for the ejecting and remaining phase $F_{AR}(t) = (P_{VL}(t) - P_W(t))/(R_{VL2\,AR} + Z_{AR0})$, while for the filling and iso-volumetric phase $F_{AR}(t) = 0$; (2) With the flows through the resistances being known, the flow into the capacitances follow by application of the fact that flows add to zero in each node. For example: $F_{CAR}(t) = F_{AR}(t) - F_C(t)$. Finally, the volume of a capacitance at time t is found by integration of the flow from the starting point of the simulation up to time t taking the initial condition regarding the volume into account.

The parameters of the model were tuned so that the model mimics the hemodynamic characteristics of either a control[14] or HFpEF and HFrEF as summarized in Table 1. The numerical values assigned to the parameters in the model (see Fig. A.1 for reference) are given in Table A2. Simulation results with these parameter values are shown in Figure 2.